RESEARCH PAPER

Modified Patch Search-Based Advanced Compressive Sensing for Efficient Colour Image Recovery: Study on Set14 Benchmark

Tejaswini Chetty[1], Anshuj Jain[2], Paresh Rawat[3], Laxmi Singh[4] and Ravishanker Choudri[5]

[1,2,3,4]ECE, Rabindranath Tagore University, Bhopal, India
[5]ME, SISTec, RGPV, Bhopal, India
[1]tejuchoudri@gmail.com, [2]anshuj@sgsuniversity.ac.in, [3]parrawat@gmail.com, [4]laxmi.singh@aisect university.ac.in and [5]rvchoudri@gmail.com

Received: 24th April, 2026; Revised: 20th May 2026; Accepted: 30th June, 2026; Available Online: 10th July, 2026

ABSTRACT
Compressive Sensing (CS) has been an area of active research in image acquisition and reconstruction even with scarce datasets, particularly in low-data scenarios. The current hybrid reconstruction approaches do not perform well in the low compression ratio scenario, with over-blurring and over-smoothing and feature loss and accuracy of reconstruction resulting from excessive iterations. To overcome these challenges the study introduces a restricted-iteration Group Sparse Representation (GSR) approach to the problem which reduces over-smoothing while capturing key image structures. This method is applied for the luminance aspect of the Y-Cb-Cr color space and uses a modified mean-distance metric to enhance patch matching. Additionally, a hybrid sparse compressive sensing framework named HLSB-RGSR is proposed by combining an Adaptively Learned Sparsifying Basis (ALSB) with the proposed restricted GSR approach. The reconstruction process was optimized by Monte Carlo simulations. The modified patch search approach focuses on finding similarity between patches by taking advantage of disparities in mean intensity. Experimental results show that it improves significantly at low compression ratios (0.1 and 0.2). The results show that unlike MH-BCS-SPL, ALSB, GSR, and HRCoGSR, the proposed HLSB-RGSR offers a better reconstruction quality, achieving an average PSNR boost of 1.15–2.12 dB while maintaining efficient recovery performance compared to our state-of-the-art alternatives.

Keywords: Image Compressive sensing**,** CS applications, Image reconstruction, GSR, ALSB, TV-NLR, HRCoGSR, HLSB-RGSR, PSNR

How to cite this article: Chetty T, Jain A, Rawat P, Singh L, Choudri R, Modified Patch Search-Based Advanced Compressive Sensing for Efficient Colour Image Recovery: Study on Set14 Benchmark. Int J Drug Deliv Technol. 2026;16(7): 945-965; DOI: 10.25258/ijddt.16.7.102
Source of support: Nil.
Conflict of interest: None

1. INTRODUCTION

Hybrid Sparse Compressive Sensing (H-SCS) is an advanced signal processing technique that integrates compressive sensing and sparse representation principles to reconstruct signals with fewer measurements than traditional methods. This approach exploits the sparsity of many signals across multiple domains, particularly those with inherent structures such as audio and images. This process involves acquiring a limited number of linear measurements, estimating the signal coefficients in various sparse domains, and merging these estimated coefficients to recreate the original signal. H-SCS gives good noise resistance, smaller sampling rates, precise reconstruction accuracy. Applications are: image and video processing, medical imaging, radar and sonar systems, wireless communication. Recent proposed works of Zhou C, et al. (2022), which hybridize distinct group sparse representation strategies with total-variation techniques resulting in improved outcomes.

Table 1 Nomenclature used for the study

Short form	Abbreviation	Short form	Abbreviation
CS	Compressive Sensing	FT	Fourier Transform
HCS	Hybrid Compressive Sensing	DWT	Discrete Wavelet Transform
ALSB	Adaptively Learned Sparsifying Basis	DDWT	Dual-Tree Discrete Wavelet Transform
GSR	Group Sparse Representation	DCT	Discrete Cosine Transform
TV-NLR		SWT	
PSNR	Peak Signal to Noise Ratio	DFT	Discrete Fourier Transform
SBI	Split Bregman iteration	JPEG	
ASNR	adaptive sparse non local regularization	GSNN	Graph Sparse Neural Networks

**Author for Correspondence: tejuchoudri@gmail.com*

BCS	Block Compressive Sensing	ESRR	Exact Sparse Representation Recovery
BP	Basis Pursuit	BLASSO	
OMP	Orthogonal Matching Pursuit	CNN	Convolutional Neural Network
BCS-SPL	Smoothed Projected-Landweber- Block Compressive Sensing	CT	Contour let Transform
MH-BCS-SPL	Multi-Hypothesis Smoothed Projected-Landweber- Block Compressive Sensing	HSI	Hyper Spectral Image
RCoS	Recovery with Collaborative Sparsity	LMF	Local Matrix Feature
GSR-JR	group sparse representation with joint regularization	ZSGSR	Z-score standardized group sparse representation
EEG	Electroencephalogram	ICSR	
SWIFTNET		NLTV	Nonlocal total variation
DISCOS		JPG-SR	Joint patch-group-based sparse representation
SAR	Synthetic Aperture Radar	LGSR	Lp-norm group-based sparse representation
WSN	Wireless Sensor Network	LSM	Learning-based sensing matrix
IoUT	Internet of Underwater Things	HSV	Hue saturation and value
H-SCS	hybrid sparse compressive sensing	MS-GSRC	Multi-Scale Group Sparse Residual Constraint Model

But hybrid methods suffer from factors such as longer processing times, particularly for color images, and having difficulty selecting the best sparse model. Moreover, they could cause over-smoothing and blurry images. The need for imaging data makes transmission via wireless challenging since the bandwidth of data sources and system-related delays. Compressive sensing has been used to compress image data, although research limitations persist. Various abbreviations used for current research article are presented in Table 1.

1.1 Motivations

The Adaptively Learned Sparsifying Basis (ALSB) mechanism plays a crucial role in enhancing compressive sensing reconstruction by dynamically learning an optimal dictionary tailored to the intrinsic characteristics of the input image. Unlike conventional approaches that rely on fixed, pre-defined dictionaries, ALSB constructs an adaptive dictionary D from image patches, enabling a more accurate and sparse representation of the underlying image structure. This is achieved by jointly optimizing the dictionary $D$and sparse coefficients $a_k$under the constraint $S_k = Da_k$with sparsity regularization $\| a_k \|_p \leq L$, where $p \in \{0,1\}$. Such adaptive modeling significantly improves representation fidelity, as the learned basis functions are closely aligned with the true image content rather than generic features. As a result, ALSB inherently suppresses noise by filtering out components that do not conform to the learned sparse structure, thereby reducing noise amplification commonly observed in fixed-dictionary methods. Furthermore, within the HLSB-RGSR framework, ALSB serves as a stabilizing initial reconstruction phase by iteratively monitoring PSNR to detect convergence and prevent unnecessary updates that could introduce artifacts. This ensures preservation of essential image details while achieving early stabilization. The use of ℓ_0-based sparsity further strengthens this process by promoting highly compact representations. Consequently, ALSB establishes a high-quality and noise-resilient reconstruction baseline, which facilitates more effective refinement in subsequent restricted GSR stages, ultimately leading to improved reconstruction accuracy without overfitting or excessive smoothing. However, it can be observed that when hybrid combination Group Sparse Representation (GSR) based compressed sensing (CS) methods work at sub-rates as low as 0.1 or 0.2, their performance significantly decreases. These three things lead into decreasing image performance as well due to overfitting, too much noise, and misalignment of the image versus existing dictionary. A conventional GSR method typically has 120 loops and can degrade this performance further, due to lack of data, causing blurry images. It picks up noise instead of solid references. Hybrid GSR also suffers from this issue, filtering away details even more when images are fragmented into patches. Most techniques also use fixed dictionaries, which results in less accurate results. Adaptive dictionaries that fit with the data, and reconstruction systems that are smarter must help us find better outputs for compressed images. Overfitting due to standard GSR has been observed in the traditional GSR model, for which the authors presented Restricted GSR methodology, where the growth of PSNR during image reconstruction ceases at a certain point. This is where improvements do not occur, leading to fitting noise rather than the actual signal features. Unlike standard GSR techniques, which usually utilize a fixed maximum number of iterations (for example 120 iterations), this new approach proposes that the system monitor PSNR and stop the process once significant growth halts. Experiments reported that this critical point occurs around 35 iterations, and should be taken as a limit.

Recovery of data is the primary difficulty, as most means to recover data are slow. Hybrid approaches (such as group sparse representation, or block compressive sensing) are also considered which could enhance the recovery quality especially for colour images that are represented differently from each other. The hybrid approach achieves better outcomes in expensive or inefficient data collections. It makes high-quality reconstruction with fewer measurements by virtue of maintaining signal sparsity across domains, which is useful for various applications. J. Zhang et al. proposed a novel framework for image compressive sensing (CS) based on adaptively learned sparsifying basis (ALSB) to enhance the sparsification of natural images using overlapping patches. This method directly addresses the non-convex L0 minimization problem, resulting in improved CS recovery. A technique based on Split Bregman iteration (SBI) was developed for efficient optimization with an average PSNR improvement of 6.2 dB and greater visual quality. Zhiyuan Zha et al. put forward the adaptive sparse non-local regularization based (ASNR) methodology which involves ALSB and GSR for the hybrid colour image CS, investigates the image quality of different attacks and compares elapsed time and memory requirements. The explosive growth of 2D image data has introduced storage and transmission challenges and necessitates a lot of memory and bandwidth. With this, it has initiated the investigation on solutions such as Compressive Sensing (CS), that provides an economical method to sample and compress signals with fewer measurements as discussed in Upadhyaya et al. [4] (2020). CS enables faster sensing at low sampling rates. Of CS techniques Block Compressive Sensing (BCS) is a common choice for 2D image processing because it works with equal-sized non-overlapping blocks, which can lead to block artifacts. In an attempt to mitigate this, Sanjay M Belgaonkar [5] proposed a CS framework based on Basis Pursuit and Orthogonal Matching Pursuit algorithms; OMP achieved the best results. S. Mun et al. [6] proposed the BCS-SPL reconstruction algorithm to reduce artifacts but the reconstructed images were still susceptible to suboptimal quality due to Wiener filtering and fixed convergence speed.

Total Variation-based minimization is a popular technique to recover natural images because of its edge-preservation, but disadvantages include texture issues and staircase artifacts. There are several approaches by which researchers have advanced image compressive sensing recovery. TV-NLR was presented by J. Zhang et al. as one of the approaches to suppress staircase effects and retain details. C. Chen developed the MH-BCS-SPL model to overcome block artifacts and enhance reconstruction. The SNR performance of Zhou's MH method was lower. Zhang et al. developed the RCoS technique that is iterative and slow to converge, being susceptible to blurry outputs. J. Zhang's framework applies L0 minimization to eliminate artifacts and improve performance, but is also slow in recovery. Liu, Z et al. developed the Wiener filtering [13], but still have difficulties reaching an appropriate patch size for various imaging types. J. Zhang et al. [14] proposed the GSR model that has improved image reconstruction by the use of image blocks of comparable structures and SVD. J. Zhang also advanced GSR by using nonlocal patches to generate a sparse representation of normal images so that it can preserve local sparsity and nonlocal self-similarity. Lee, S et al. [15] proposed a novel model for the recovery of blurred images affected by Cauchy noise with an alternating optimization method and unique initialization. Wang R et al. [16] presented the GSR-JR model that is the best compromise between sparsity and complexity in image reconstruction. This article focuses on the area of hybrid CS and calls for more research around scalability, robustness to noise, and efficient algorithms for real-time applications. H-SCS is expected to keep growing in different areas of research.

1.2 Contribution of Work

This study has focused on examining various hybrid CS methods, challenges, and open issues in recent research. The authors proposed a fast and efficient H-SCS approach that combines the benefits of an adaptive learned sparsifying bas and GSR approaches. The prime contribution of research is to design fast and accurate reconstruction method especially for colour images in order to save the significant memory utilization. Method also helps to maintain the structural similarity of recovered images. Since accurate signal reconstruction primarily depends on the development of efficient algorithms in terms of measurement matrix and sensitive to noise and distortion. Therefore, this paper contributes to identify the challenges and limitations of existing works of CS methodologies. As a major contributions paper presents the case study to GSR, hybrid CS and machine learning CS based methods on brief survey. Major challenges in CS algorithm are achieving higher accuracy in signal reconstruction along with future scope are discussed. Paper also presets scope for open future research. Major contribution of retrench is to propose the modified patch search method using man difference error distance. this can preserve the patch feather and improves the structure similarities. The proposed method introduces a novel approach to image reconstruction by combining the strengths of Markov Chain Monte Carlo (MC) sampling with group sparse representation (GSR). This integration leverages the probabilistic nature of MC to explore the solution space effectively while utilizing GSR to capture intrinsic image structures and dependencies. By incorporating a dictionary-based regularization term, the algorithm enhances its ability to preserve fine details and textures in the reconstructed image. The iterative refinement process, alternating between MC sampling and GSR optimization, allows for progressive improvement of the reconstruction quality. This unique combination of techniques addresses limitations of existing methods and potentially offers improved performance in terms of reconstruction accuracy and computational efficiency.

2. RELATED WORK

CS is the most widely used field in image processing and has a large scope. The versatile applications of CS techniques in signal processing are illustrated in Figure 1, which serves as a visual representation of its fundamental technology. The Figure 1 consists of eight hexagonal elements, each depicting a distinct area of application: wireless sensor networks, biomedical imaging, satellite communications, biometric authentication, video processing, speech processing, dimension reduction, and hardware implementations. CS finds its use across various sectors including healthcare, communication, security, and computer hardware. The visual layout of this information is straightforward and easily comprehensible, making it an effective resource for educational or presentational purposes.

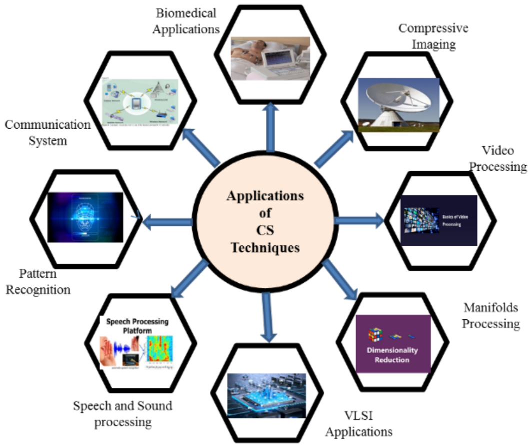

Figure 1 Frequently used CS Applications

Compressive sensing techniques has significant applications across various fields, including audio, image processing, computer vision, cognitive radio, and wireless sensor networks. Different applications necessitate specific sensors and communication technologies. Key imaging techniques utilizing CS are medical, satellite, infrared, and underwater imaging are as shown in figure 2, where CS improves image quality, reduces scan times, enhances resolution, increases sensitivity, and minimizes noise

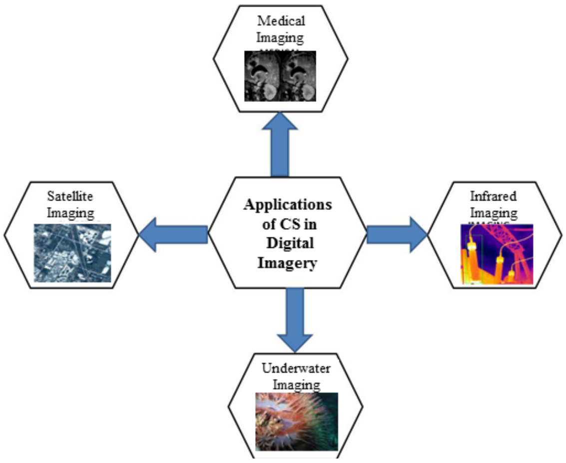

Figure 2 Applications of CS on different Images

2.1 Block Compressive Sensing (BCS)

Block compressive sensing (BCS) extends traditional compressive sensing (CS) by recovering sparse or compressible signals from fewer measurements. BCS typically consists of partitioning inputs into blocks for discrete measurements. Important contributions are made by Hou et al. [17] techniques for hyperspectral images, which enhance the estimation of noise variance; Wang, Z et al. [18] parallel BCS employing partial DFT and DCT; Monika et al.[19] discussion on difficulties of data transfer that need pre-processing; Y. Gu et al.[20] refinement for elemental image arrays; Mishra et al.[21] multi-focus image fusion technique, which effectively combines BCS with projection-driven reconstruction; and Li et al.[22] BCS_PGDNET, which employs an neural network to improve recovery of image sub-blocks.

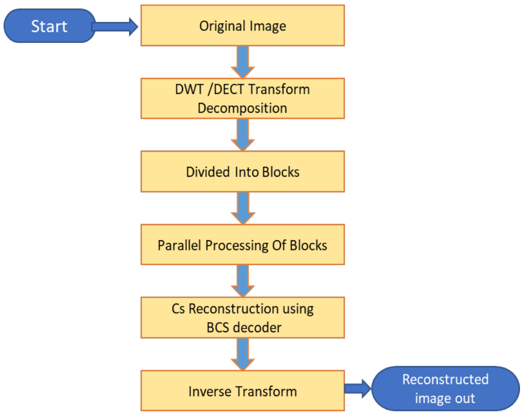

Figure 3 Flows of BCS

Their study compared this method with several existing algorithms, showing superior image reconstruction in terms of both accuracy and speed. The process of sequential BCS based reconstruction is illustrated in Figure 3. It is clear that using different combination of transform decomposition, BCS iteratively reconstruct images.

2.2 Transformation based Methods

The categories of the several BCS-based techniques are displayed in Figure 4. The transformation-based methods are the focus of the categorization diagram. Discrete cosine-based transform (DCT), discrete wavelet-based transform (DWT & DDWT) are the primary transformations utilized to improve the performance of BCS techniques.

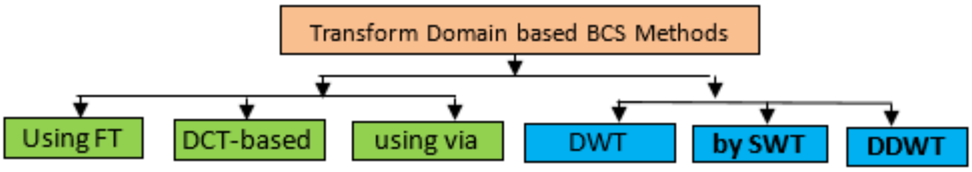

Figure 4 Classification chart for the various transform domain based BCS methods

Two of the most well-known types of these directional transforms are contourlets and complex-valued DWTs. The CT, or contourlet transform, preserves appealing qualities of the conventional DWT, including multiresolution and local signal characteristics, and it better captures the directional characteristics of the image, despite the expense of spatial redundancy. The CT maintains the Laplacian pyramid's redundancy while combining Laplacian pyramid decomposition with directional filter banks. Due to the simplicity of its implementation, the dual-tree DWT (DTDWT) has gained popularity as a method for complex-valued wavelet transforms, which have been presented as an alternative to overcome DWT flaws. The real-valued wavelet filters of the DDWT generate the transform's real and imaginary parts in parallel decomposition trees. The DDWT is an overall redundant tight frame because both of its trees are orthonormal or biorthogonal decompositions, although the traditional DWT's decomposition has a lower level of directionality than the DDWT's decomposition.

2.3 Challenges of Recent Compressive Sensing Methods

This paper explores the implementation of Compressive Sensing (CS) in image processing and some issues faced by CS. These have to do with the coherence considerations of accurate reconstruction, large area network applications, low energy clustering design for wireless sensor networks (WSN), WSN algorithms based on different distances, as well as problems with scaling. The issues highlighted in Figure 5 are: computational complexity; over-smoothing and noise amplification; loss of color information; and hardware constraints. These constraints prevent CS from being used in real-time and thus affect the speed and accuracy of it. Thus, establishing a quick, efficient, and content-preserving CS is necessary.

Figure 5. Challenges of Compressive Sensing

As illustrate in Figure 5 that CS methods used for colour images may loss the colour information and are sensitive to blur in reconstructed image. Thus, its challenge to still improve the quality of colour images CS. in this context this research paper prosed to investigate the new design of hybrid colour image CS technique.

4. RESEARCH GAPS AND FEATURES OF HYBRID GSR METHODS

To improve the performance and address the limitations of traditional compressive sensing, hybrid compressive sensing (HCS) was introduced. HCS is a combination of traditional compressive sensing (CS) techniques and other signal processing methods. Some of the key research gaps and features are shown in Figure 6.

Research Gaps

Figure 6 shows major research gaps concerning CS-based image recovery. These factors indicate 6 major limitations of current reconstruction methods: reduced performance at low compression ratios, over-smoothing and loss of image details, noise amplification with reconstruction artifacts and color information loss; high computational complexity and processing time; inaccurate patch similarity measurement in Group Sparse Representation (GSR)-based recovery; and the difficulty of sparsity basis adaptation for diverse image content.

a) Major research gaps b) Hybrid GSR based features

Figure.6 Research Gaps and features of the Hybrid GSR based CS

Such issues hamper the quality of reconstruction and increase the computational cost and narrow the applicability of existing CS-based approaches, mainly in low-sampling, noisy, and real-time image recovery conditions. Filling these research gaps is critical towards achieving more robust, precise and efficient compressive sensing image reconstruction schemes. So far in CS of patch-based GSR, the current GSR approaches have a severe limitation on matching patch similarity measurement: the reliance on standard Euclidean distance methods to estimate similarity does not allow for lighting invariance while assessing structurally similar patches at best. This neglect particularly runs the risk of undermining the very basis of patch-based reconstruction on images with varying illumination conditions: similar patches may be reasonably well-matched up and sparsely represented.

3. PROPOSED DESIGN METHODOLOGY (H-ALSB-RGSR)

Leveraging existing ANSB and adapted Restricted GSR-based HLSB-RGSR schemes, this research presented a hybrid CS strategy that provides a fundamentally new reconstruction architecture as compared to previous studies. This integrates their diverse merits into a single, three-phase optimization model. Our proposed approach enables better detail preservation without compromising denoising, in contrast to the ALSB model, which has worked well against reconstruction noise, but loses fine details of the image at low compression ratios (e.g., we obtained just 25.8852 dB PSNR of the Leaves image with a sub-rate of 0.1). Although structural data and sharp edges are well preserved with group-wise sparse representation, typical GSR techniques often yield over-smoothed and blurry reconstructions, as a result of a static iteration approach regardless of the sampling ratio. Such limitations can be overcome with the HLSB-RGSR framework applying a three-phase sequential reconstruction process.

Pre-processing: Moving the input picture from the sRGB domain to the perceptually uniform Y-Cb-Cr; colour space improves the statistical representation for compressive sensing. The resulting signal's sparsity is improved and its coefficient distribution in subsequent transform domains is more instructive by separating the luminance component, which contains the majority of the structural information, from chromatic changes. By lowering redundancy and improving entropy characteristics, this preprocessing step increases the amount of helpful information available for reconstruction and makes it easier to recover from a small number of compressive measurements with greater accuracy and stability.

MH-BCS-SPL: During the initial stage, the Modified Multi Hypothesis based Hybrid MH-BCS-SPL algorithm is utilized to derive a dependable preliminary assessment of the image based on the compressive measurements. The initialization captures the main low-frequency structures while retaining important edges and textures by carefully choosing the discrete wavelet transform breakdown level (usually 2 or 3) at MH stage along with the search-window size w. This initial reconstruction of superior quality acts as an educated beginning for the following refinement phases, quickening convergence, raising stability, and ultimately raising the accuracy of the picture that was eventually recovered.

ALSB Phase: To avoid excessive noise, this Adaptive Learning-Based Sparsifying Basis (ALSB) learns an image-adaptive dictionary in the second stage, while monitoring the reconstruction quality with the Peak Signal-to-Noise Ratio (PSNR). Finally, in the third step, we propose a Restricted Group Sparse Representation (R-GSR) method, which adaptively restricts the number of sparse reconstruction iterations to avoid extensive smoothing while preserving structural elements and fine textures. Moreover, instead of the classic Euclidean distance metric, the proposed method employs a new mean-intensity-adjusted patch similarity statistic. The proposed metric also compensates for lighting variation, allowing for more precise grouping of structurally similar patches, since they can be cantered by mean subtraction prior to estimation. Improved patch matching increases sparse representation accuracy, reduces reconstruction artifacts, and retains high-frequency picture data.

The proposed research to improve the performance of reconstruction quality and to speed up the recovery process proposed a restricted adaptive CS approach. Figure 7 illustrates the proposed block diagram of the hybrid H-ALSB-R-GSR compressive sensing system.

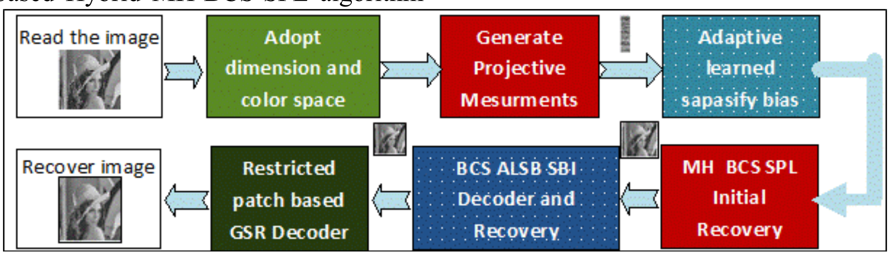

Figure 7 Proposed block diagram of hybrid H-ALSB-R-GSR compressive sensing

The proposed hybrid process as in Figure 7, begins with reading an image, followed by selecting a particular dimension and colour space. The protective measurements were performed using the BCS method. The image is then reconstructed in sequence using the proposed hybrid three-stage approach. The compressed measurements were processed with an adaptive learned sparsify bias, and an initial estimate was generated using a multi-hypothesis (MH)-based decoder. The decoded image was subsequently processed further by a BCS ALSB SBI decoder for recovery in the release series if a restricted iterative patch-based R-GSR decoder was applied. The proposed method adaptively achieves rapid performance and optimal PSNR. The entire process exemplifies a hybrid approach to compressive sensing that combines multiple techniques for improved image reconstruction. The proposed hybrid approach takes advantage of adaptive learned sparsity bias and also the patch-based group reconstruction. The ALSB incorporation at pre phase of compressive sensing improves image reconstruction quality, optimizes the reconstruction process, and it is also faster compared to other methods like RoCs (A. Jain et al). Compared to other methods of state of art proposed ALSB based per recovery phase contributes to efficient compression while maintaining high reconstruction quality. The combination of restricted R-GSR based CS with adaptive LSB hybrid method leverages the strengths of both techniques to enhance image reconstruction quality and efficiency. By utilizing patch-based group reconstruction from GSR and the adaptive learning capabilities of ALSB, this combined approach achieves efficient compression while maintaining high reconstruction quality. The pre-recovery phase contribution of ALSB-based processing further enhances the overall performance, making this hybrid method a promising solution for advanced image reconstruction tasks. The proposed HLSB-RGSR framework is capable of achieving an average PSNR enhancement of 1.15–2.12 dB over different sampling ratios.

3.1 Proposed H-ALSB-RGSR Modelling

The research improves patch similarity by tweaking the way patches are compared. Instead of using plain Euclidean distance—which usually gets thrown off by lighting changes—the method subtracts the average intensity from each patch before comparing them. Let B and Vrepresent two image patches (or vectors) of size N, write

$$d_{\text{eq}} = \sum_{i=1}^{N} (B_i - V_i)^2 \quad (1)$$

While simple and computationally robust, the Euclidean distance presumes that two patches of the same image have nearly identical pixel intensities. However, this assumption is often violated in real photos because changes in local illumination, sensor exposure, shadows, and brightness may modulate intensity values without substantially affecting the underlying structural information. Thus, simply their average brightness difference can lead to a large Euclidean distance between two patches that reflect the same texture or edge. Frequently, resulting patch groupings are not aligned with their original intent, which then leads to suboptimal image reconstructions and sparse representation. This restriction is overcome with our suggested technique, which introduces a mean-intensity-adjusted patch similarity measure by removing the mean intensity of each patch before calculating the similarity distance. This small change basically canters all patches, making sure differences in lighting across an image don't mess up the comparison. The proposed similarity metric is written as follows:

$$d_{\text{ZMSSD}} = \sum_{i=1}^{N} [(B_i - \bar{B}) - (V_i - \bar{V})]^2 \quad (2)$$

where: d_{ZMSSD} stands for zero-mean sum of squared differences. The intensity levels for the i-th pixel in reference as well as candidate patches are denoted by B_i an V_i, respectively. The reference and candidate patches' mean intensity levels are denoted by B and V respectively. The total number of pixels in each patch is denoted by N.

Excluding overall brightness effects improves resolution, and thus, allows a stronger focus on the underlying structure and texture of each patch, thus allowing more accurate grouping of similar patches. Using singular value decomposition in GSR, notably in the Hybrid HLSB-GSR method, produces cleaner results that maintain detailed information while reducing noise and artifacts. In practice, tests show that an increase in PSNR of one-to-two dB is achieved and structural similarity is improved. For the HLSB-RGSR method, a complex multi-step solution involving incremental repetition balancing noise reduction with detail preservation is supported by the concept of the adaptive ALSB technique which stabilizes reconstruction and minimizes visible noise while preserving detail. Phase three presents the Restricted GSR method based on nonlocal similarities in order to improve the reconstruction accuracy. CS techniques focus on colour images, and are based on their signal sparsity and mathematical optimization approach, which is different from conventional sampling approaches.

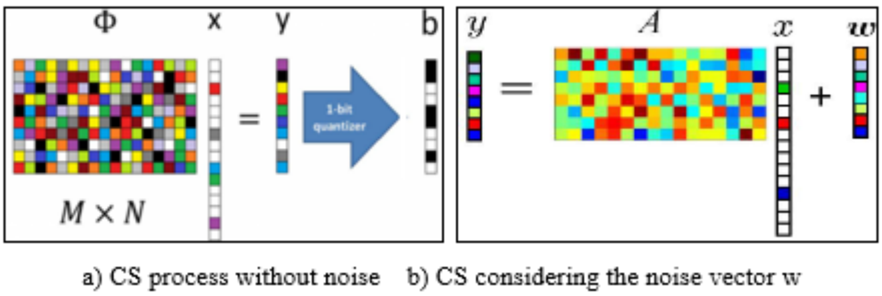

Figure 8 Sparsity and the image CS process with and without using noise models

This paper proposed noise free CS model. Figure 8 illustrates a sparse recovery technique based on single vector CS. Based on the fundamental sparse one vector model seen in Figure 8 a). The Figure 8 a) shows that the signal can be compressed to create the sparse representation by applying basic matrix manipulation as well as transformation techniques. The formulation may be based on the idea of linear projection, which asserts that each compressed measurement is created as a weighted linear combination of all image pixels. The i^{th} measurement is given by:

$$y_{\mathrm{i}} = \Sigma_{j=1}{}^{\mathrm{N}} \varphi_{ij} x_j, \quad i = 1, 2, \ldots, M \tag{3}$$

where φ_{ij} may represent the $(i, j)^{th}$ element of sensing matrix as Φ. By combining all the measurements into a single vector, the sensing process can be finally written as:

$$\mathrm{y} = \Phi\mathrm{x} = \mathrm{b} \tag{4}$$

where $\mathrm{x} \in N$ is the original signal or picture patch, b is the measurement vector matching to the n-th block (or patch), $\mathrm{y} \in \mathrm{R}^{\Phi}$ is the compressed measurement vector, and $\Phi \in \mathrm{R}^{q_b \times N}$is is the sensing (measurement) matrix.

. The notation b indicates that the measurement vector consists of compressed samples corresponding to the selected measurement indices q_β. These measurements retain the essential structural information of the original image while substantially reducing the amount of acquired data. This reduction lowers storage requirements, minimizes transmission bandwidth, and accelerates image acquisition without significantly compromising reconstruction quality. As illustrated in Figure 8 b), the sparse vector model that includes noise consideration where the y is sparse signal, ϕ is the random sample vector non orthogonal projection matrix of image. The x is the observed measurements with without considering the noise. $b_{n \in q_b}$is the quantized result with n=1 bit. It can be observed from the Figure 8 a), that using the simple matrix manipulation and transformation functions can compress the signal to generate the sparse representation. Acquired data in real-world compressive sensing (CS) systems are bound to be impacted by a variety of noise sources that occur during the process of obtaining, detecting, transferring, and imperfect hardware. Thus, the optimum measurement model is expanded to take into account the impact of measurement noise. The noisy CS the sparse one vector model with consideration of noise vector W as shown in the Figure 8 b) can be models as;

$$y = A * x + W \tag{5}$$

where; $y \in R^{\mathrm{M}}$ denotes the observation vector, $A \in R^{\mathrm{MxN}}$ denotes the sensing (measurement) matrix, $x \in R^{\mathrm{N}}$ denotes the original image signal, and $W \in R^{\mathrm{M}}$ denotes the additive noise vector. The linear projection of the high-dimensional image into a lower-dimensional measurement space is carried out by the sensing matrix A, and the noise vector represents the mistakes made throughout the sensing operation. The encoder of CS-based image compression is less computationally complex and independent of the image signal, which is one of its main advantages. Using a hybrid recovery strategy is the primary way to address the problem of recovering images from sparse data. Our suggested approach, which uses adaptive learning sparsifying basis via l_0 reduction, for image compressive sensing recovery is expressed as

$$\hat{\mathrm{x}}_{\mathrm{org}} = \mathrm{D} \arg\min \alpha \left\{ \frac{1}{2} \parallel \mathrm{y} - \Phi \mathrm{D}\alpha \parallel_2^2 + \lambda \parallel \alpha \parallel_0 \right\} \tag{6}$$

where α is the sparse coefficient vector, λ is the regularization parameter that controls sparsity, y is the measurement vector, Φ is the sensing matrix, D is the dictionary matrix, and $\hat{\mathrm{x}}_{\mathrm{org}}$ represents the original image (or signal) that has been recreated.

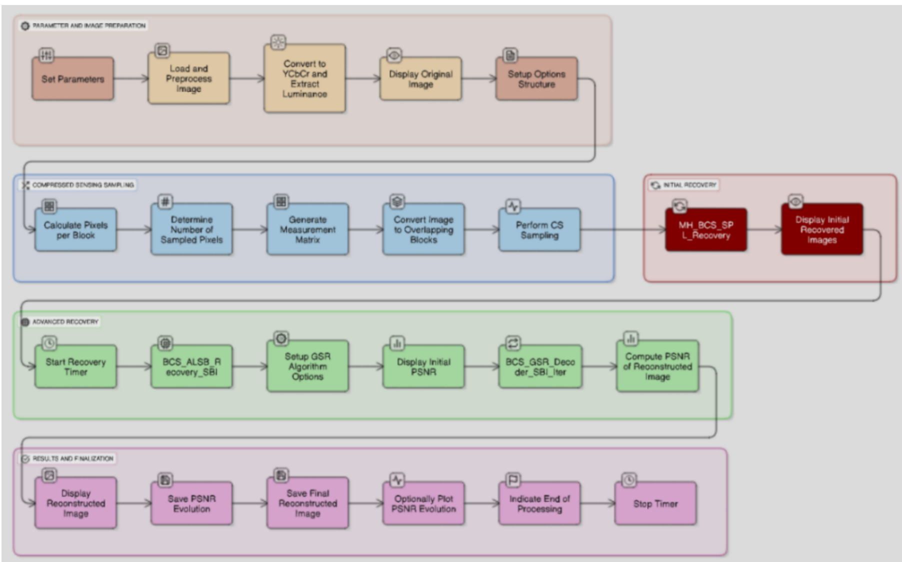

Figure 9 Proposed Block diagram of hybrid CS methodology

Algorithm 1: Hybrid Adaptive H-ALSB-RGSR CS
1. Initialization: set compression ration or sub rate R, Block size B. and iteration number 2. Loop through Images: for Img_{No} = 4 for Sub rate = 0.4 3. Read image X_{Org} 4. Dimension adoption and 2D conversion ←gray,← RGB 5. Convert it to Y-Cb-Cr colour space.← separate Y image 6. Compress image using eq. (1) **7. Recovery Phase Initializations** a. Number of iterations for ALSB. b. ALSB threshold (← Th= 10). c. Determine the number of sampled pixels $\quad \mathrm{M} = \mathrm{round}(\mathrm{Subrate} * \mathrm{B}^2 \quad (7)$ 8. Image recover using MH-BCS-SPL $$(\widehat{X})mh = arg\min_X(\|Y - \Phi X\|\frac{2}{2} + \lambda \sum i \|\psi_i(X)\|_1) \qquad (8)$$ 9. Apply the ALSB based recover of images 10. calculate the PSNR for every iteration and evaluate 11. restore Img_{ALSB} to further processing 12. Apply the Restricted GSR phase to solve the optimization problem as $$min_\alpha \| Img_{ALSB} \|_0 \qquad (9)$$ 13. calculate the PSNR for every iteration and evaluate
End Algorithm

The combination of MH-ALSB-and restricted GSR based decoders are proposed in this work to optimally solve the eq. and preserve the information in recover image better. The flow chart of the proposed method is illustrated in the Figure 9. the respective sequential description is given in the Algorithm 1

3.2 Adaptive learning-based sparsifying bas

The selection of the dictionary of sparsifying bas D is crucial for sparse representation models. Stated differently, how can one determine which domain is optimal for sparsifying the particular image under sensing. Learning the redundant scarifying foundation from a collection of training example picture patches has been a major focus. In compressive sensing (CS), it is critical to represent image patches with a sparse collection of coefficients in the right transform domain to produce excellent image reconstruction. Conventional transforms like the Discrete Cosine Transform (DCT) and Wavelet Transform offer sparse representations, but they utilize set basis functions that fail to adequately capture the varied local structures, textures, and edges found in natural photographs. Therefore, a successful option is adaptive dictionary learning, which involves learning the sparsifying basis straight from the image data. By enhancing reconstruction precision and maintaining delicate image features, this adaptive approach produces a redundant sparsifying basis (dictionary) that is specifically suited to the image's inherent qualities. Take into account a collection of J overlapping training picture patches that were taken from the input image,

$$S = [S_1, S_2, \dots, S_j] \qquad (10)$$

where; a column vector represents each picture patch $S_k \in R^n$. According to the theory of sparse representation, every image patch may be roughly expressed as a linear combination of just few atoms chosen from an overcomplete dictionary $D \in R^{n \times K}$, with $K > n$. Consequently, each training patch is represented as follows

$$S_k \approx Da_k \qquad (11)$$

where; a_k represents the sparse coefficient vector for the k^{th} picture patch and D stands for the adaptive sparsifying dictionary. Since the dictionary is overcomplete, the same image patch might be represented by numerous sparse coefficient vectors. Therefore, sparsity is enforced by limiting the number of active coefficients, which is expressed as follows:

$$\|a_k\|_p \leq L, \quad where\ p = 0\ or\ 1 \qquad (12)$$

where; L is the highest allowed sparsity level, $\|a_k\|_0$ is the amount of non-zero coefficients, and $\|a_k\|_1$ is the sum of the absolute values of the coefficients. The l_0-norm enforces precise sparsity, whereas the l_1-norm offers a convex relaxation that is computationally more manageable. In adaptive dictionary learning, the goal is to determine the optimal dictionary D and the sparse coefficient matrix.

$$\Lambda = [a_1, a_2, \ldots, a_j] \quad (13)$$

Dictionary Learning Algorithm

Since the adaptive dictionary D and the sparse coefficient matrix Λ are both unknown, an alternating optimization method is utilized for the dictionary learning process. To optimize the method, two sequential steps must be executed. Sparse coding applies an Iterative Hard Thresholding (IHT), Orthogonal Matching Pursuit (OMP), or Basis Pursuit (BP) algorithm to the image patch to determine the sparse coefficients to minimize the rebuilding error due to the sparsity constraint. The second step of the dictionary update is to enhance the dictionary atoms, for example K-SVD, Method of Optimal Directions (MOD), adaptive least-squares optimization, etc., to maintain the sparse coefficients constant. These two processes are repeated alternately until reconstruction error converges or reaches the maximum number of iterations, and an adaptive dictionary is obtained that accurately represents the structural characteristics of the image, which provides compact, efficient, and sparse representation, and the reconstruction error is reduced. In order to minimize the approximation error during the reconstruction of each image patch while adhering to the sparsity restriction. The iterative dictionary learning process can be summarized by the following optimization equation:

$$(\widehat{\mathrm{D}}, \widehat{\mathrm{A}}) = \arg\min \mathrm{D},\ \mathrm{A} \sum_{k=1}^{J} \| \mathrm{s}_k - \mathrm{Da}_k \|_2^2 \text{ subject to } \| \mathrm{a}_k \|_0 \leq L, \forall\, k \quad (14)$$

where; J is the total number of training samples, L is the sparsity constraint, s_k is the k-th training image patch, a_k is the corresponding sparse coefficient vector, $\widehat{\mathrm{D}}$ and $\widehat{\mathrm{A}}$ represent the learned dictionary and sparse coefficient matrix, respectively. In Eq. (14) the objective function consists of two complementary components. The first component.

$$\Sigma_{k=1}{}^{J} \|S_k - Da_k\|^2{}_2 \quad (15)$$

Is also dubbed the data fidelity term or reconstruction error. It determines the Euclidean distance between the original image patches and their reconstructed equivalents. This error may be reduced, allowing the dictionary that has been learned to correctly portray image edges, textures, and structural data. The other element;

$$\|a_k\|_p \leq L \quad (16)$$

Is the sparsity constraint, which restricts the number of active dictionary atoms used in reconstructing each patch. This constraint eliminates redundant coefficients, suppresses noise, avoids overfitting, and ensures compact image representations. Consequently, the learned dictionary adapts to the statistical characteristics of the image while maintaining sparse and efficient representations. For natural images, patch-based sparse representation mathematically denoted by $\mathbf{x} \in \mathrm{R}^N$ and subset $\mathrm{x}_k \in \mathrm{R}^{B_s}$. The original image's vector representations and a size-based image patch $\sqrt{B_s}$ X $\sqrt{B_s}$ at location k, k = 1, 2, …., ɳ. This leads to;

$$x_k = R_K \boldsymbol{x}, \quad (17)$$

Where, $R_K \in R^{B_s\ X\ N}$ represents a matrix operator to extract patches $\boldsymbol{x_k}$ from $\boldsymbol{x}$. Keep in mind that patches typically overlap, making this type of patch-based representation extremely repetitive. During this phase the convergence criterion is maximum number of iterations predefined as 35 maximum number of iterations. This criterion guarantees computational efficiency and prevents unnecessary processing once acceptable convergence has been achieved

3.3 Patch based GSR

In the next phase the performance improvement is achieved with combining the LSB approach with GSR based on patch-based approach. The recovered LSB image is further segmented into overlapping patches, and patches exhibiting similarity are subsequently grouped. For each of these groups, the following optimization problem is addressed**:**

$$min_\alpha \ \| \alpha \|_0 \ \ subject\ to \ \ \| Y - \Phi D\alpha \|_2^2 \ \leq \epsilon \quad (18)$$

Where:

- D denotes dictionary that encapsulates the basic functions utilized for sparse representation.
- α represents sparse coefficient vector associated with the selected elements from dictionary.
- ϵ signifies the error tolerance, which ensures that the reconstructed signal closely approximates the observed measurements.

The problem is solved using detailed algorithm for Restricted GSR is given in Algorithm 2.

Algorithm 2: **Restricted GSR Recovery:**
1. Read the image X_{alsb} : recovered final image from ALSB phase *2. Perform split Benjamin iteration (SBI) until the iteration count reaches a predetermined maximum*

defined by the BCS-GSR-SBI-Decoding algorithm.

3. for *t=1:35* At each iteration *t*
4. Update the estimate ← $u^{\wedge}: u^{\wedge} = u^{\wedge}(t) + \mu(p_u - y + \mu(u^{\wedge} - D_C{}^{\circ}\alpha - b))$ (10)
5. *Update the bias term b*
6. Evaluate the PSNR for each iteration as

$$PSNR = 10log10\left(\frac{MAX^2}{MSE}\right). \quad (11)$$

7. Do until stopping criterion max (ITR) is satisfied.
8. learn from the PSNR pattern to set the limit to ITR=t.
9. end Algorithm

As clear from the Algorithm 2 that method update of the signal estimate, denoted as $u^{\wedge}$, is formulated through an iterative process that incorporates various components critical to signal reconstruction. The equation expresses the new estimate $u^{\wedge}$ at iteration t as a function of the current estimate $u^{\wedge}(t)$, the prior estimate pupu, and the observed measurements y. It also integrates the dictionary matrix $D_C{}^{\circ}$, which is applied to the sparse representation, alongside the sparse coefficient vector α and a bias term b. The learning rate, represented by μ, governs the adjustment magnitude in response to the differences between the reconstructed signal and the observed data, thereby refining the estimate iteratively to enhance accuracy and convergence towards the true signal.

4. RESULTS AND DISCUSSION

The input images data base used for the current study is shown in the Figure 10 where vessels image is of size 96 x96, and all other images are of 256x256 size. The colour images are first converted from RGB to Y-Cb-Cr. and the only Y component is further processed. the vessels image is of size 96 x96, and all other are of size 256x256 including colour images.

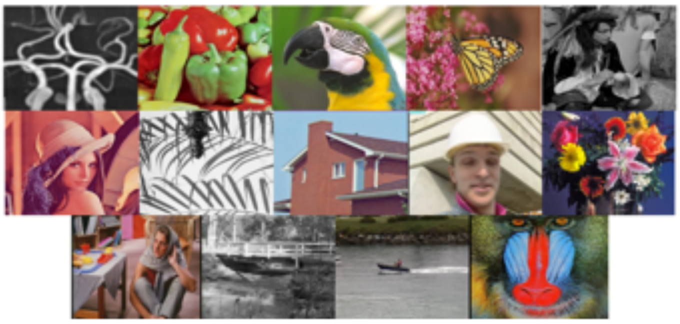

a) Set 14 images

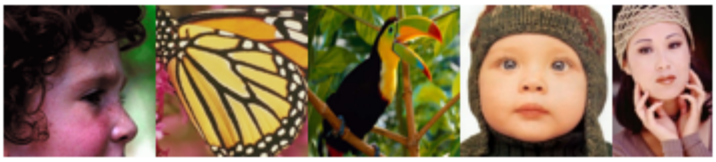

b) Set 5 images

Figure 10 Input Set14 and Set 5 test images datasets are used for the current study

The Set14 dataset contains 14 benchmark images as in Figure 10 a) used for image processing and compressive sensing experiments. The dataset includes House256rgb, Parrots, Leaves256, and Vessels96, all of size 256×256. Baboon, Barabara, Lena, Man, Pepper, and Monarch are of size 512×512 (with Monarch also having a 512×768 version depending on the dataset variant). Foreman and Coastguard are 288×352 images, while Flowers is 362×500 and Barbara is 576×720, representing higher-resolution content. Generalizability u tested on Set 5 dataset as given in Figure 10 b). Set5 is a extensively utilized benchmark dataset for image restoration and compressive sensing, consisting of five high-quality grayscale images showcasing varied textures, edges, and structural features. Because of its wide variety and moderate size, it is ideal for quantitatively assessing reconstruction fidelity and comparing the effectiveness of competing compressive sensing algorithms available at https://github.com/linzino7/Set5-dataset. These images collectively provide a mix of low, medium, and high-resolution scenes for evaluating reconstruction algorithms. The proposed algorithm results are evaluated in the three [phase as phase I -III.

Phase I: the initial estimate of the recovered full-size image is achieved by the use of MH-BCS-SPL based decoder. this decoder uses the wavelet transform decompositions for recovery. where MH represented the Multi Hypothesis method, BCS is block-based CS approach and SPL is smoothed projected-Landweber

(SPL) iterative reconstruction. Method is fast but offers in ideal lower PSNR estimate.

Phase II: this phase is implemented using the extension of ALSB approach and is iterated to achieve the PSNR and recovery quality improvement.

Phase III: This phase is final restricted GSR (R-GSR) based decoder using SBI (Split Bregman Iteration) approach. the conventia0onal GSR offers 120 iterations by default. but as an observation the most of time after a certain iterations PSNR remains stable. thus, restricting the iterations may achieve the fast and better recovery of images. this phase competed the proposed approach of image recovery with HLSB-RGSR approach.

4.1 Experimental Evaluation and Discussion

The validation results presented in Figure 11 illustrate the Peak Signal-to-Noise Ratio (PSNR) outcomes for two methodologies—Adaptive Least Squares Basis (ALSB) and Group-based Sparse Representation (GSR)—applied to vessel and leaf images. the Table 2 presented the all-default values used for the variables in proposed method.

Table 2 variables description and range

Variable	Description	Default Value
X	Original image matrix	Not specified
Φ	Measurement matrix	M×N matrix (where M<N)
Y	Compressed measurements	$Y=\Phi XY$
X_{MH}	Initial reconstructed image	Output of MH-BCS-SPL algorithm
Λ	Regularization parameter	0.1
R(X)	Regularization term	0.01
D	Dictionary for GSR	Predefined dictionary (e.g., learned from training data)
A	Sparse representation	0.5
ϵ	Error tolerance for GSR	0.01
M	Number of rows in Φ	M<N
N	Number of columns in Φ (vectorized image block size)	N>M

The results are validated and the PSNR patters are compared for three different sub rates as [0.4, 0.2 and 0.1] for vessels and Leaves Images as illustrated in the Figure 11. For the Vessels images as in Figure 11, the ALSB method achieved a PSNR of 37.81 dB at a rate R=0.4, indicating lower performance in reconstructing for the image compared to GSR, which recorded a PSNR of 40.56 dB under the same conditions. It is also observed that as the sub rate decreases the performance of ALSB is lagging compared to GSR. This slight difference underscores the effectiveness of GSR in maintaining higher fidelity during reconstruction.

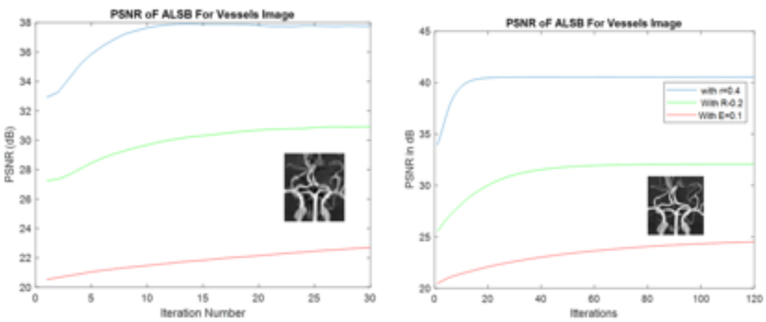

a) Validation of the PSNR for ALSB (40.88 dB at R=0.4)

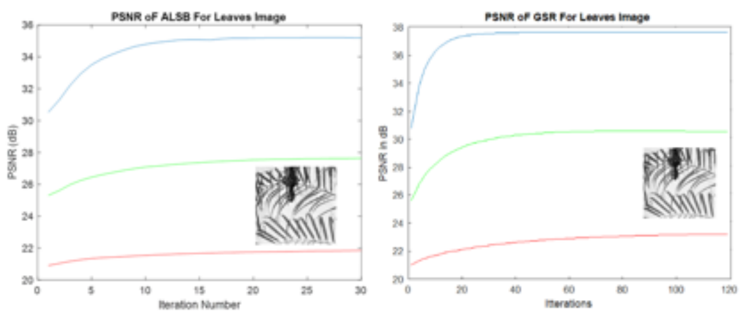

b) Validation of PSNR for GSR Existing (40.56 dB at R=0.4)

Figure 11 Results of the Validation of PSNR for the CS methodology for the Vessels image

In this experiment, 35 iterations were used for ALSB and 120 iterations for GSR. The PSNR values for Leaves images show that ALSB achieved 35.19 dB at R=0.4, while GSR achieved 37.83 dB. It is suggested to utilize both methodologies based on their comparable performance. Figure 12 compares image recovery results for leaves and vessels using the ALSB method. For leaves, PSNR values for ALSB are 25.8852 dB, 27.4772 dB, and 35.1912 dB at R values of 0.1, 0.2, and 0.4, indicating decreased image quality with increased sub rate. The GSR method shows a maximum PSNR of 36.346 dB at R=0.4, outperforming ALSB but is prone to over-blurring. For vessels, ALSB yields PSNR values of 37.7627 dB, 30.9233 dB, and 22.6982 dB for R=0.4, 0.2, and 0.1, while GSR achieves 40.4684 dB, 31.504 dB, and 22.664 dB, respectively.

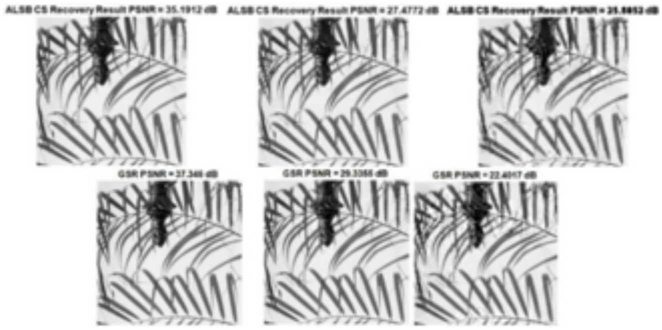

a) comparative results for Leaves Image for different sub rates

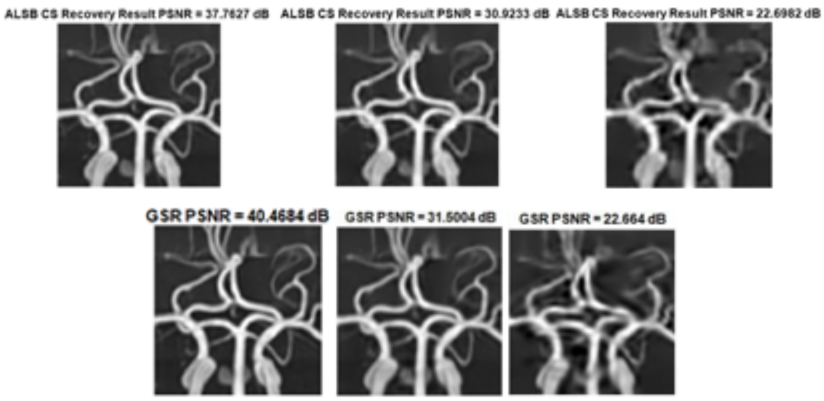

b) comparative results for Vessels Image for different sub rates

Figure 12 Comparative results of the ALSB and GSR as Validated for R=0.4,0.2 and 0.1 a) first row for Leaves image, b) row two for Vessel's image

Thus, GSR outperform over existing ALSB. but at the lower compression ration as the requirement of most of applications overall performance still needs improvement. it is a demand to design a method which equally performs on each range of sub rates. Thus, this paper has proposed a novel hybrid approach for performance improvement.

4.2 Results of Proposed HLSB-RGSR Approach

This section presented the comparative results of our hybrid proposed method. The first phase has presented the qualitative and quantitative results of our proposed method HLSB-RGSR. The results of the comparative analysis of image reconstruction quality by the proposed method phase III for PSNR and reconstructed images are presented in Figure 13. The results for R=0.1, 0.2, and 0.4 in the Vessels image (96x96) size indicate that the proposed hybrid method HLSB-RGSR phase III provides a notable improvement in PSNR. The red boxes highlight regions of interest for evaluating image recovery quality, showing reduced blurriness at higher Sub rates. Overall, the boxes assist in visually comparing reconstruction quality across various methods and parameters.

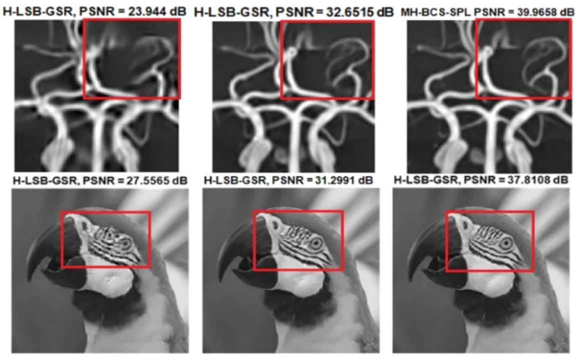

a) for R=0.1 b) for R= 0.2 c) for R=0.4

Figure 13 Proposed results of hybrid combination of H-LSB-RGSR with patch-based approach for the Vessels and Parrot images

The results presented in Figure 13 illustrate that the proposed method effectively generates high-quality images for vessels and Parrot images at sub rates R=0.1, 0.2, and 0.4, achieving PSNR values of 23.944 dB, 32.6515 dB, and 39.9658 dB respectively for vessels, and 27.5565 dB, 31.2991 dB, and 37.8108 dB for Parrot images. The Parrot image, originally in RGB, was converted to Y-Cb-Cr color space to apply the recovery method on the Y component to preserve color information. Figure 14 displays a comparison of PSNR values against iteration counts for the hybrid approach of Phases II and III, showing that higher sub rates correspond to improved PSNR performance. Notably, the proposed method maintains higher PSNR values even at lower sub rates due to its hybrid approach, with optimized iteration counts set at a ratio of 35-35 for the two phases.

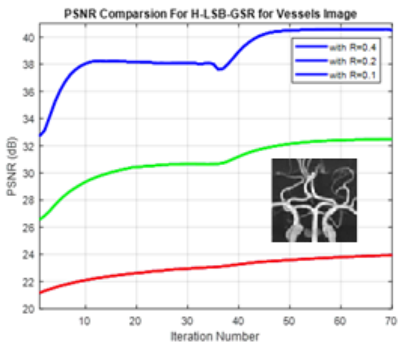

a) for Vessels Image 1:70 Iterations

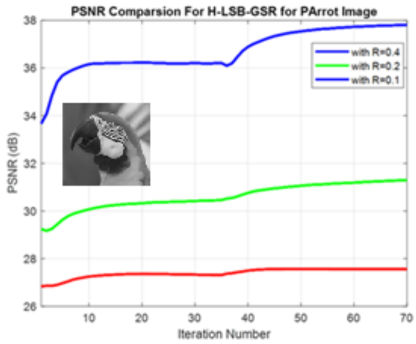

b) for Parrot Image 1:70 Iterations

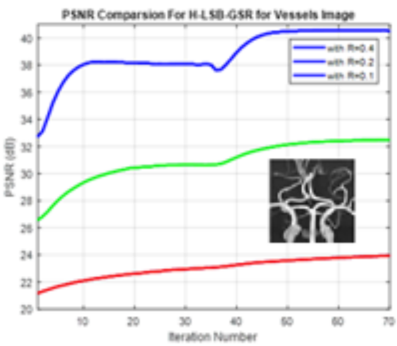

a) for Vessels Image 1:70 Iterations

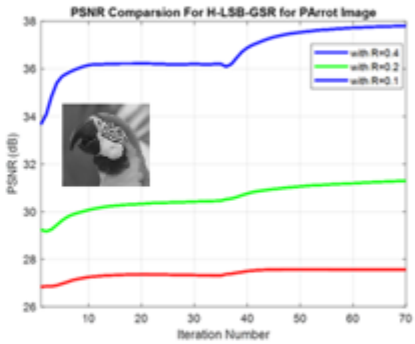

b) for Parrot Image 1:70 Iterations

Figure 14 Quantitative performance evaluation of the Proposed HLSB-RGSR Approach

The slight dip around iteration ~35 in your Hybrid HLSB-GSR PSNR curve is actually a common phenomenon in iterative sparse reconstruction algorithms. It does not indicate failure—in fact, it often reflects an internal transition in the optimization process. It is due to shift of proposed method from LSB phase to GSR phase. It is since the GSR reconsidered the recovered output of LSB phase and 36-70 iterations belongs to modified patch search based GSR where patch similarity groups are computed. The Figure 14 a) presented the results for the three sub rates for vessels image. While the Figure 14 b) represented the results for the Parrot image. These results make it clears that recovered image quality is significantly increased. the slight dip and rise pattern at the 35 iterations is signifying the shift and transfer of outcomes of Phase II ALSB to the final phase as restricted GSR. it can be observed that after the nearly 20 iterations the GSR PSNR nearly become stable.

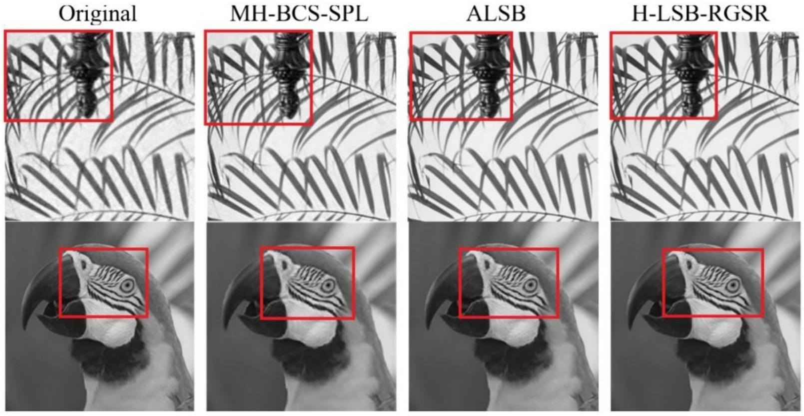

Figure 15 Qualitative comparison results of the proposed HLSB-RGSR approach

The Figure 15 has displayed a qualitative evaluation of the proposed image recovery results. The study compares different image recovery results at Phase I , Phase II and Phase III if the proposed hybrid approach. The sub rates are varied for 0.1, 0.2 and 0.4. The ALSB technique effectively smooths out noise, while proposed H-LSB-RGSR maintains sharper details while reducing noise. The choice of the best denoising technique depends on the specific application and trade-off between noise reduction and detail preservation.

Table 3 State of art methods comparison and Quantitative performance measure as PSNR in dB vs sub rates

Image	Sub rates	GSR J. Zhang, [14]	HNLSR . Li, Lizhao [24]	HRCoGSR (Phase-I) Jain, Abjishek [23]	Proposed Phase 1 MH-BCS-SPL	Proposed Phase II ALSB	Proposed HLSB-RGSR Phase III
Vessels	0.4	40.4684	**40.620**	38.6201	33.060	38.02	40.1991
	0.2	31.5004	**33.1601**	30.2602	25.881	30.923	32.587
	0.1	22.664	22.560	**24.660**	19.7302	22.11	23.077
Leaves	0.4	34.461	**38.551**	38.0102	29.91	34.942	37.1889
	0.2	30.601	29.030	**30.9701**	25.30	27.68	30.1624
	0.1	22.4017	22.661	**24.5401**	20.89	25.8852	23.6609
Parrot	0.4	36.51	36.19	33.67	34.58	36.21	**37.6028**
	0.2	31.17	31.41	29.90	30.23	31.14	**32.1329**
	0.1	26.37	27.22	26.68	27.23	27.58	**27.9542**
Barbara	0.4	38.991	39.1602	34.8201	33.17	37.310	**39.2898**
	0.2	34.69	33.8901	29.620	30.99	31.69	**34.6907**
	0.1	28.20	28.771	25.8902	26.8201	26.491	**29.4408**
Lena	0.4	36.48	36.82	36.40	37.53	38.84	**39.5197**
	0.2	31.36	31.57	31.65	34.10	34.93	**35.7962**
	0.1	27.56	28.04	27.84	30.95	31.29	**32.19**
Peppers	0.4	37.21	37.87	*39.99*	37.05	38.18	**38.388**
	0.2	30.83	31.19	*33.87*	35.72	36.86	**34.1476**
	0.1	26.01	27.91	*26.87*	31.52	32.73	**33.4391**
House	0.4	40.89	41.87	***44.84***	38.76	41.35	42.2235
	0.2	37.03	36.98	***40.13***	33.85	35.93	37.34
	0.1	33.46	33.58	*34.77*	31.47	34.12	**34.9248**
T test		**32.32655**	**31.8729**	**32.57148**	**30.54217**	**33.04707**	**34.09109**

Based on Table 3, the proposed HLSB-RGSR Phase III method demonstrates superior PSNR performance compared to various state-of-the-art methods. It consistently achieves competitive or superior PSNR values for images such as Vessels, Leaves, Parrot, Barbara, and Lena, particularly outperforming others at sub-rates of 0.2 and 0.1. The T-test results of 33.02399 confirm a statistically significant improvement in PSNR, reinforcing the method's superiority in performance.

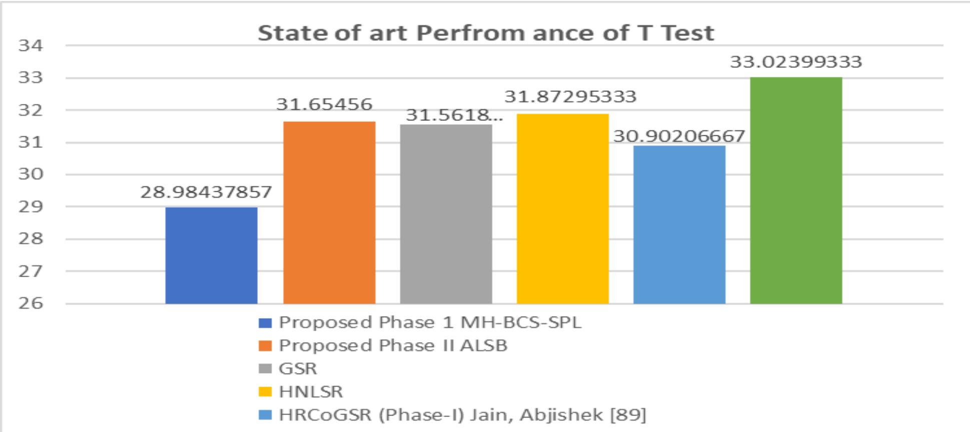

Figure 16 State of art performance comparison for T test.

The T test performance is represented clearly in the bar chart as in Figure 16. The T-test results further substantiate the performance of the proposed method, with a score of 33.02399, the highest among all methods evaluated. This suggests that the proposed method provides a statistically significant improvement in PSNR compared to its counterparts. It is clear the proposed method offers the 1.15109 dB average improvement over HNLSR and 2.1219 dB gain over recent HCoGSR methods. it is because that proposed modified method offers the consistent improvement in the in final phase for lower sub rates of 0.2 and 0.1.

T-test Evaluation: The Table 3 illustrates that the proposed HLSB-RGSR (Phase III) method gets the greatest average PSNR (34.09 dB), demonstrating better reconstruction fidelity than the rival techniques. The same collection of image/sub-rate pairs (n=21, 20 degrees of freedom) should undergo a paired t-test using the paired PSNR disparities between each baseline and HLSB-RGSR. When the p-value is less than the predetermined significance level (usually 0.05) and the confidence interval for the mean difference does not include zero, statistical significance is shown. Such a conclusion would demonstrate that the observed PSNR increases are probably the result of the hybrid framework's real improvement rather than chance. By giving rigorous statistical support for the proposed approach's supremacy and by complementing the numerical improvements observed across all images and sampling rates, we may report the precise t-statistics, p-values, and 95% confidence intervals for each pairwise comparison.

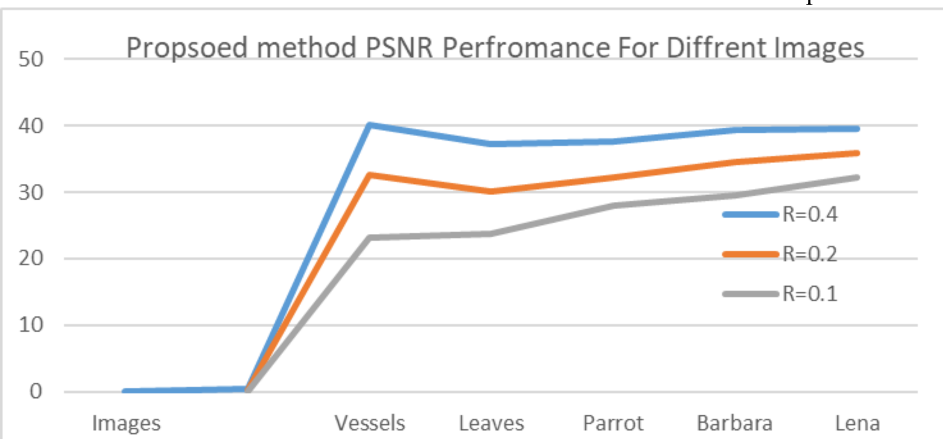

Figure 18 Performance comparison of Proposed HLSB-RGSR for different images

Figure 18 have presented the line graph for the performance comparison of proposed HLSB-RGSR for different images. It is clear the Vessels, Lena, and Barbara images offers good results for all three sub rates.

4.3 Results of Generalizability and Ablation study on Set 5 dataset

This section has presented the result of the generalizability tested open the Set5 image dataset and the three evaluations matrix are used as PSNR, structural similarity index (SSIM) (SSIM) and Visual Information Fidelity (VIF) index defined as;

$$\mathrm{SSIM}(x, y) = \frac{(2\mu_x\mu_y + C_1)(2\sigma_{xy} + C_2)}{(\mu_x^2 + \mu_y^2 + C_1)(\sigma_x^2 + \sigma_y^2 + C_2)},$$

and

$$\mathrm{VIF} = \frac{\sum_{j} \sum_{i} I(C_{i,j}; F_{i,j} \mid z_{i,j})}{\sum_{j} \sum_{i} I(C_{i,j}; E_{i,j} \mid z_{i,j})},$$

The VIF quantifies the fraction of visual information preserved in the distorted image relative to the reference image.

The simulations are run for the three different sampling ratio as [R=0.1, 0.2 and 0.4] for the Set5 image data as Babyx2 and Buterflyx2 as .png images. The graphical comparative results are shown in the Figure 18. It shows that the hybrid approach that was suggested is applicable to a variety of image characteristics. At the greatest sampling ratio (R=0.4), the peak values for the butterfly image are around 30.3 dB PSNR, 0.98 SSIM, and 0.65 VIF. The approach achieves around 37.1 dB PSNR, 0.97 SSIM, and 0.75 VIF for the Baby×2 image as well. The algorithm efficiently maintains both smooth regions and fine textures, as shown by the monotonic rise in PSNR with increasing sampling ratio, together with the constantly great visual information fidelity and structural similarity.

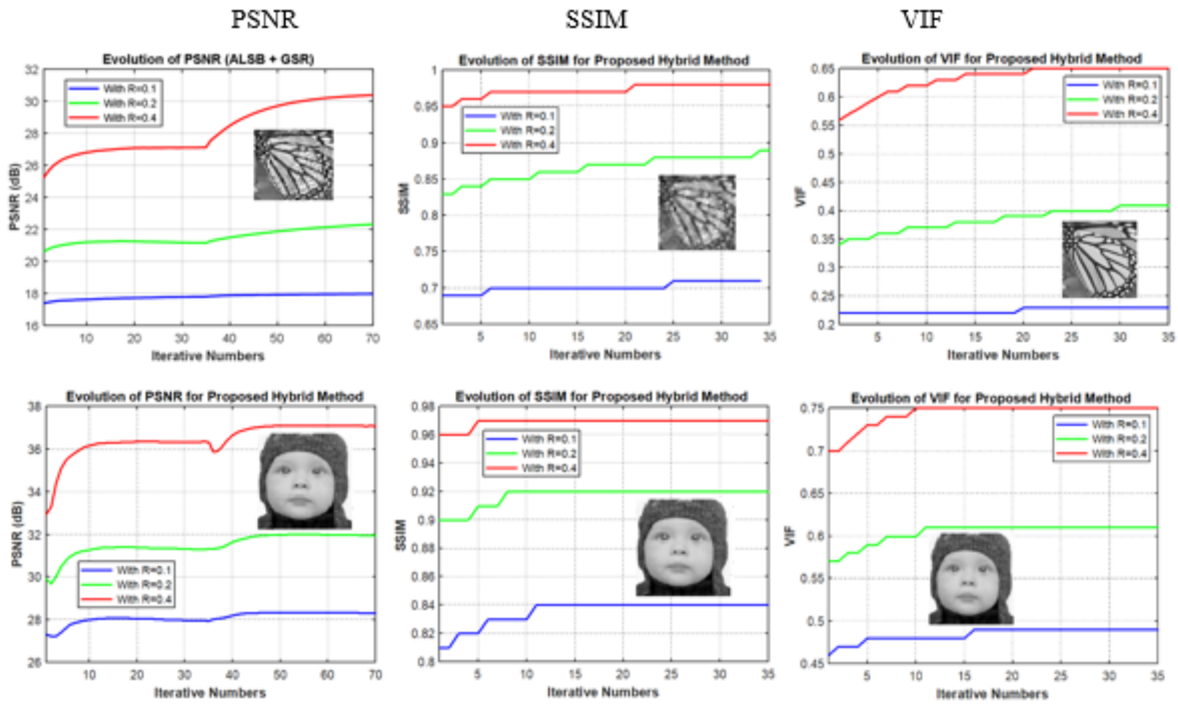

Figure 18 Generalizability test results tested on Set 5 database

The robustness and generalizability of the proposed reconstruction framework beyond the training or development set are strongly supported by the high peak metric values and comparable convergence behaviour on these visually dissimilar test images.

Figure 19 Ablation study comparative results a) Vessel image b) TV-NLR 22.60 dB, c) MH 25.12 dB, d) proposed MH-BCS-SPL Phase I 25.881 dB, e) ALSB Phase II 30.9223 dB, f) GSR 31.5004 dB g) HLSB-RGSR Phase III 32.587 dB

The ablation study in Figure 19 demonstrates a consistent improvement in reconstruction quality as successive components of the proposed framework are incorporated. The baseline TV–NLR method achieves 22.60 dB, while the inclusion of the MH strategy increases the PSNR to 25.12 dB. Introducing the Phase I MH-BCS-SPL module further improves the performance to 25.881 dB. A substantial gain is obtained with the ALSB module in Phase II (30.9223 dB), followed by an additional enhancement through GSR (31.5004 dB). The complete Phase III HLSB-RGSR framework attains the highest PSNR of 32.587 dB, representing an overall improvement of nearly 10 dB over the baseline. These progressive gains verify that each stage contributes positively to image reconstruction, while the superior performance of the full model confirms the complementary nature and effectiveness of all proposed components, thereby justifying the ablation study.

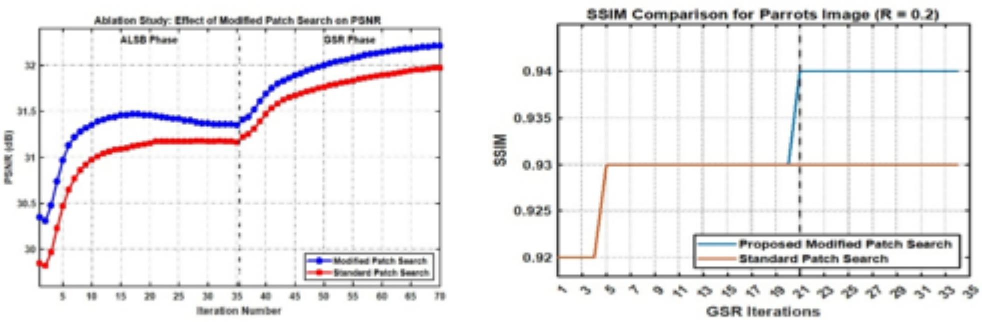

Figure 20. (a)Ablation study of Modified patch search PSNR results (b) Comparision of SSIM values of parrot image(R=0.2)

The figure 20(a) shows the ablation study by replacing the standard patch search with the proposed modified patch search consistently increases PSNR throughout both the ALSB and GSR phases, yielding an overall improvement of approximately 0.24 dB in final reconstruction quality, thereby confirming the individual contribution of the proposed patch search strategy.

The figure 20(b) demonstrates that the proposed modified patch search consistently achieves higher structural similarity than the standard patch search. While the conventional approach stabilizes at an SSIM of approximately **0.93**, the proposed method further improves the SSIM to **0.94** during GSR refinement, confirming its effectiveness in preserving image structures and enhancing perceptual reconstruction quality.

Figure 21 demonstrates that the proposed HLSB-RGSR Phase III method consistently outperforms ALSB throughout the iterative process and converges to a higher PSNR. For $R = 0.1$, the final PSNR increases from approximately 27.94 dB (ALSB) to 28.31 dB (HLSB-RGSR), corresponding to a relative improvement of about **1.3%**. For the less compressive case $R = 0.4$, the final PSNR rises from about 36.35 dB to 37.08 dB, yielding a relative improvement of approximately **2.0%**.

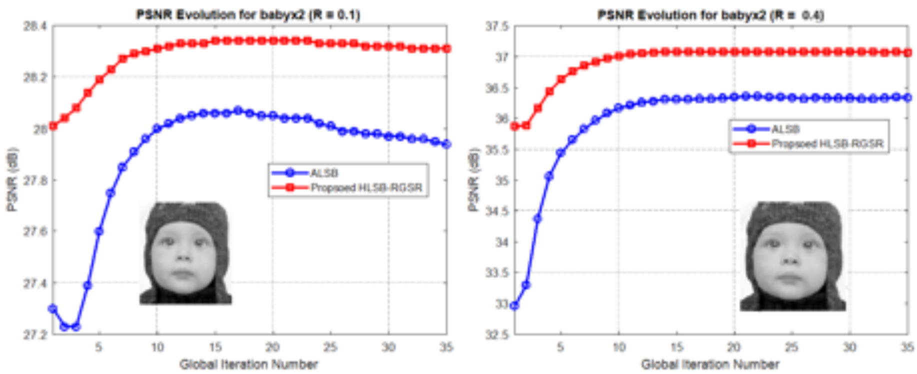

Figure 21 Parametric ablation study results for existing ALSB and proposed HLSB-RGSR Phase III approach a) for the R=0.1 b) for R=0.4

Overall. the smooth and rapid convergence of the proposed approach, together with its consistently superior reconstruction quality at both sampling ratios, confirms the effectiveness of the additional HLSB and RGSR components and thereby justifies the parametric ablation study.

5. CONCLUSION AND FUTURE SCOPE

The hybrid least squares blending–regularized generalized sparse representation (HLSB-RGSR) framework combines a modified Adaptive Least Squares Blending strategy with Generalized Sparse Representation and provides robust and accurate compressive sensing image reconstruction while mitigating overfitting through a limited number of iterations. The proposed technique was compared with recent state-of-the-art reconstruction algorithms based on a thorough study of existing compressive sensing algorithms and their design challenges to have stable performance. In comparison, HLSB-RGSR achieved the best PSNR results with very diverse images and sampling sub-rates and performed well especially at low sampling ratios of 0.1 and 0.2, with the most informative signal components being specifically targeted. The adaptive weighting mechanism of ALSB and the sparse modeling capability of GSR improve noise robustness of the model while maintaining fine features in the image during image recovery. Statistical validation using paired t-tests concluded that the proposed Phase III hybrid method outperformed the competing methods, with p-values below

0.05 indicating significant PSNR improvements over the competing methods available. On average HLSB-RGSR induces PSNR enhancement of around 1.15 dB compared to HNLSR and 2.12 dB compared to the latest HCoGSR method. Furthermore, a higher sampling ratio to 0.3 and 0.4 improves SSIM and VIF scores, quickens convergence time, and provides improvement in structural fidelity and stability. The uniform evolution of these results for both textured and smooth grayscale images, like House, Foreman, and Monarch and the color images like Lena, Parrot and Barbara, is indicative of the good generalizability and performance of the proposed reconstruction procedure. Future work will focus on validating the HLSB-RGSR framework on larger and more diverse image datasets, including hyperspectral and medical images, to further establish its robustness and generalizability.

REFERENCES

[1] Zhou, C., Kong, Y., Zhang, C., Sun, L., Wu, D., and Zhou, C. “A Hybrid Sparse Representation Model for Image Restoration.” *Sensors* 22, no. 2 (2022): 537.

[2] Zhang, J., Zhao, C., Zhao, D., and Gao, W. “Image Compressive Sensing Recovery Using Adaptively Learned Sparsifying Basis via L0 Minimization.” *Signal Processing* 103 (2014): 114–126.

[3] Zha, Z., Liu, X., Zhang, X., Chen, Y., Tang, L., Bai, Y., Wang, Q., and Shang, Z. “Compressed Sensing Image Reconstruction via Adaptive Sparse Nonlocal Regularization.” *The Visual Computer* 32, no. 9 (2016): 1239–1253.

[4] Upadhyaya, V., and Salim, M. “Compressive Sensing: An Efficient Approach for Image Compression and Recovery.” In *Recent Trends in Communication and Intelligent Systems*, 25–36. Singapore: Springer, 2020.

[5] Belgaonkar, S. M., and Singh, V. “Image Compression and Reconstruction in Compressive Sensing Paradigm.” *Global Transitions Proceedings* 3, no. 1 (2022): 220–224.

[6] Mun, S., and Fowler, J. E. “Block Compressed Sensing of Images Using Directional Transforms.” In *Proceedings of the International Conference on Image Processing*, 3021–3024. Cairo, Egypt, 2009.

[7] Sun, L., Wen, X., Lei, M., Xu, H., Zhu, J., and Wei, Y. “Signal Reconstruction Based on Block Compressed Sensing.” In *Artificial Intelligence and Computational Intelligence*, 317–324. Berlin: Springer, 2011.

[8] Li, C., Yin, W., and Zhang, Y. “TVAL3: TV Minimization by Augmented Lagrangian and Alternating Direction Algorithm.” Technical Report, 2009.

[9] Zhang, J., Liu, S., Xiong, R., Ma, S., and Zhao, D. “Improved Total Variation Based Image Compressive Sensing Recovery by Nonlocal Regularization.” In *2013 IEEE International Symposium on Circuits and Systems (ISCAS)*, 2836–2839. Beijing, China, 2013.

[10] Chen, C., Tramel, E. W., and Fowler, J. E. “Compressed-Sensing Recovery of Images and Video Using Multi-Hypothesis Predictions.” In *Proceedings of the Asilomar Conference on Signals, Systems and Computers*, 1193–1198. Pacific Grove, California, 2011.

[11] Zhou, C., Chen, C., Zhang, Y., Ding, F., and Zhang, D. “MH-Net: A Learnable Multi-Hypothesis Network for Compressed Video Sensing.” *IEEE Access* 7 (2019): 169023–169034.

[12] Zhang, J., Zhao, D., Chen, Z., Xiong, R., Ma, S., and Gao, W. “Image Compressive Sensing Recovery via Collaborative Sparsity.” In *Proceedings of the Data Compression Conference*, 287–296. Snowbird, Utah, 2012.

[13] Liu, Z., Chen, L., and Yang, J. “An Image Reconstruction Algorithm Using Patch-Based Locally Optimal Wiener Filtering.” *Journal of Electronics and Information Technology* 36 (2014): 2556–2562.

[14] Zhang, J., Zhao, D., and Gao, W. “Group-Based Sparse Representation for Image Restoration.” *IEEE Transactions on Image Processing* 23, no. 8 (2014): 3336–3351.

[15] Lee, S., and Kang, M. “Group Sparse Representation for Restoring Blurred Images with Cauchy Noise.” *Journal of Scientific Computing* 83 (2020): Article 41.

[16] Wang, R., Qin, Y., Wang, Z., and Zheng, H. “Group-Based Sparse Representation for Compressed Sensing Image Reconstruction with Joint Regularization.” *Electronics* 11, no. 2 (2022): 182.

[17] Hou, Y., and Zhang, Y. “Effective Hyperspectral Image Block Compressed Sensing Using Three-Dimensional Wavelet Transform.” In *IEEE International Geoscience and Remote Sensing Symposium (IGARSS)*, 2973–2976. Quebec City, Canada, 2014.

[18] Wang, Z., Jiang, Y., and Chen, S. “Image Parallel Block Compressive Sensing Scheme Using DFT Measurement Matrix.” *Multimedia Tools and Applications* 82 (2023): 21561–21583.

[19] Monika, R., Samiappan, D., and Kumar, R. “Adaptive Block Compressed Sensing: A Technological Analysis and Survey on Challenges, Innovation Directions and Applications.” *Multimedia Tools and Applications* 80 (2021): 4751–4768.

[20] Gu, Y., Piao, Y., and Huang, Y. “Adaptive Block Compressed Sensing Algorithm Based on Integral Imaging.” In *2020 IEEE 3rd International*

Conference on Electronic Information and Communication Technology (ICEICT), 85–88. Shenzhen, China, 2020.

[21] V. S. U., Mishra, D., and Subrahmanyam, G. R. “Adaptive Multifocus Image Fusion Using Block Compressed Sensing with Smoothed Projected Landweber Integration in the Wavelet Domain.” *Journal of the Optical Society of America A* 33, no. 12 (2016): 2516–2525.

[22] Li, L., et al. “Block Compressed Sensing Image Reconstruction via Untrained Network Priors.” *IAENG International Journal of Computer Science* 50, no. 2 (2023).

[23] Jain, A., Swami, P. D., and Datar, A. “Dimension Adaptive Hybrid Recovery with Collaborative Group Sparse Representation Based Compressive Sensing for Colour Images.” *International Journal of Nanotechnology* 20 (2023): 361–389.

[24] Li, L., et al. “Image Compressive Sensing via Hybrid Nonlocal Sparsity Regularization.” *Sensors* 20, no. 19 (2020): 5666.

AUTHOR'S BIOGRAPHY

Tejasvini Chetty -is research scholar at RNTU Bhopal and is MTech in VLSI Design, having the research interest in VLSI and Image processing.

Dr Anshuj Jain is Ph.D. from Rabindranath Tagore University, Bhopal, in 2020. His research interests include image processing, signal processing, FPGA-based system design, VLSI, and digital communication. He has published several research papers in reputed national and international journals and conferences.

Dr Paresh Rawat - is Ph.D. from MANIT Bhopal in 2014 and has guided many research scholars. His area of interest is Signal and Image processing, Machine Learning and AI. He has published several research papers in reputed national and international journals and conferences

Dr. Laxmi Singh - is Ph.D. from Rabindranath Tagore University, Bhopal, in 2015 and has guided many research scholars. His area of interest is Signal and Image processing.Se has published several research papers in reputed national and international journals and conferences

Dr. Ravishanker V Choudri - is Ph.D. from Mewar University, Chittorgarh, in 2020 and has guided many research scholars. He has published several research papers in reputed national and international journals and conferences